A COMPARATIVE STUDY BETWEEN RHADOPHYTA AND PHYOPHTA ON BIOSORPTION OF U AND Th IN FELSITE DYKES OF EL-SIBAI AREA, CENTRAL EASTERN DESERT, EGYPT.

***Gad, N. Sh.*[*,†] *and Samaan, J. M.*[*]**
[*] *Nuclear Materials Authority of Egypt (NMA), P.O. Box 530 Maadi, Cairo, Egypt.*
[†] *E-mail address: norashenouda@yahoo.com*

ABSTRACT
Felsite dykes of El-Sibai area characterized by high content of Uranium and Thorium, two types of algae were chosen to take action on biosorption of Uranium and Thorium from felsite dykes of El-Sibai area. Represented by [Pyrophyte (Sargassum detofiulum) and Rhadophyta (Ulva Lactuca)]. Felsite dykes of El-Sibai area characterized by a high content of Thorium (Th) and Uranium (U), Sargassum detofiulum and Ulva Lactuca show biosorption capacities of (81%, 89%), for U and (77%, 88%) for Th, respectively. Therefore, it was preferable to use Ulva Lactuca on biosorption due to its high sorption than Sargassum detofiulum.

Keywords
Sargassum detofiulum, El-Sibai area, Ulva Lactuca, biosorption, Uranium, Thorium.

1. INTRODUCTION
The mechanism for metal uptake in *Ulva Lactuca* will depend on the identity of the metal, and can be either irreversible when uptake into the cell occurs through active metabolic pathways [12]. Na and K are used to maintain osmotic pressure and charge balance, while Ca is also used to stabilize *Ulva Lactuca* polysaccharide structure on its cell wall. It has been shown that other metals interact with live *Ulva Lactuca* in an active manner as well. Uptake of Cu and Cd causes a loss of K^{+1} ion and an increase of Na^{+1} ion in live *Ulva Lactuca* cells as shown in table 1, which likely occurs due to an increase in the cell wall permeability. The same metal exposure to freeze dried tissue showed no measurable change in cellular sodium or potassium concentration. Consistent between live and dead tissue, suggesting that sorption for some metals occurs through passive, non-metabolically mediated sorption. Cerium, europium, gadolinium, ytterbium and zinc sorption on *Ulva Lactuca* [10]. As active ion transport requires metabolic energy and therefore living cells, this would suggest that sorption for these metals occurs through passive ion exchange between surface functional group protons and metals. *Ulva Lactuca* has been shown to act as a cation exchange system, for example with Pb sorption on dried algal biomass columns consisting of *Ulva Lactuca*, *Janiarubens* (red alga), and *Sargassum detofiulum* (brown alga). *Ulva Lactuca* biomasses can uptake Pb and Hg nearly about 100% with capacity about (281.8 mg/g) dry algal mass [13]. Other algal species have demonstrated cation exchange behavior as well, for example the green macroalga *Enteromorpha intestinalis* and brown algae. There are two mechanisms involved in the concentration of U. The primary mechanism is ion exchange or co-precipitation of the ion with the calcium carbonate matrix, and the secondary mechanism that involves some form of complex formation with either the protein nitrogen or other component of the organic fraction. At given pH, PCO_2, and EH of seawater, U is most likely to occur as the anionic species $UO_2\ (CO_3)_3^{4-}$ (8). The U (VI) tri-carbonate is one of the most stable metal complexes in aqueous solution. It

would readily be incorporated with calcium carbonate (or undergo anion exchange reaction) in those species of algae in which calcification occurs. [6]

Table (1): Biosorption uptake by different types of Algal species.

Metal	Algal species	Biosorption capacity (mg/g)	References
Pb	*Spirogyra.*	140.00	[2]
Pb	*Ulva Lactuca*	181.82	[1]
Cd	*Sargassum*	84.70	[3]
La	*Sargassum Detofiulum*	80.47	[9]
Ce	*Sargassum Detofiulum*	84.60	[9]
Pr	*Sargassum Detofiulum*	86.60	[9]
Nd	*Sargassum Detofiulum*	86.00	[9]
Sm	*Sargassum Detofiulum*	88.70	[9]
Eu	*Sargassum Detofiulum*	70.00	[9]
Gd	*Sargassum Detofiulum*	77.40	[9]
Tb	*Sargassum Detofiulum*	77.10	[9]
La	*Ulva Lactuca*	72.90	[9]
Ce	*Ulva Lactuca*	74.00	[9]
Pr	*Ulva Lactuca*	66.10	[9]
Nd	*Ulva Lactuca*	80.20	[9]
Sm	*Ulva Lactuca*	70.00	[9]
Eu	*Ulva Lactuca*	34.50	[9]
Gd	*Ulva Lactuca*	67.40	[9]
Tb	*Ulva Lactuca*	57.40	[9]

2. MATERIALS AND METHODS

2.1. Algal Collection and Processing

Sargassum detofiulum and Ulva Lactuca were collected from Red Sea coast, Hurghada, Egypt, transferred to laboratory in labeled polyethylene bags. The samples were washed several times with de-ionized water to remove dirt, and/or other impurities present in the raw materials. They were air dried for 10 days, then grinded and sieved at the pore size of 0.5 to 1 mm >>>>>>>.

2.2. Characterization of the Algal-biosorbent Materials

Infra-red (IR) spectrum of model Naxux 670 was applied in a spectrum ranges of 400–4000 cm^{-1} for the sample to identify the functional groups in the Central National Research (CNR) and the morphological characteristics of the algal biomasses surface and the pore and particles fractions were examined under environmental scanning electron microscope (ESEM), field emission gun (FIG) in CNR.

2.3. Samples Location

Samples were collected from felsite dykes of El-Sibai area in the central eastern desert of Egypt between latitude 25º 35′ - 25 º 45′ N and longitude 34º 00′ -43º 15′ E. It covered by crystalline basement rocks [7], it composed of ophiolites (older), Arc metavolcanics, subduction related granitoids, intra-plate magmatism and (younger) hammamt meta-sediments [11]. Table 2 show the average field measured U and Th by count per Scand (cps) in different rock types in the studied area. Selected Samples of felsite dykes of El-Sibai area, was grinded to a size of 100 meshes.

Table (2): Average U (cps) and Th (cps) in the different rock of El-Sibai area.

Rock units	U(cps)	Th(cps)
Meta ultramafic (Ophiolites)	1.2	9.5
Metagabbros (Ophiolites)	2.1	11.6
Metavolcanics	3	9.3
Older granites	5.4	19.5
Biotite granites	20.9	31.8
Alkali granites	78.4	60.8
Felsite dykes*	249	875

2.4. Adsorption Experiments

In order to investigate the ability of the *Sargassum detofiulum and Ulva Lactuca* biosorbent material to recover (U and Th) from the aqueous solutions of selected samples of felsite dykes, batch experiments were conducted by contacting (U and Th) solutions with the adsorbent (1 g/l). The flasks were placed on a shaker with constant shaking for 100 rpm, and then incubated at 30˚C for 5 days. The algal biomass was washed several times as outlined in the work of [4]. Then experiment using (ESEM) and chemically to determine Uranium and Thorium concentration from the biomass. The samples were examined by (IR) and (ESEM), in the Central National Research (CNR).

2.5. Adsorption Isotherms

To determine the equation between biosorbent material (*Sargassum detofiulum and Ulva Lactuca* biosorbent material to recover (Uranium and Thorium) from the aqueous solutions of selected samples of felsite dykes of El-Sibai area by calculating the Initial and final concentrations of *Th and U* in solution which measured with Inductively Coupled Plasma-Optical Emission Spectrometry (ICP-OES 5100). The uptake amount (A) of *Th and U* due to each sample was estimated by subtracting the final concentrations (Cf) from initial concentrations (Ci) in the liquid phase expressed as the following equation [14]:

$$A = (Ci - Cf)\, V/M\, m \; [\text{mole g}^{-1}]$$

Where V is the volume of the solution, M is the atomic weight of each element, and m is the dry weight of each sample.

3. Results and Discussion

Many techniques were used to determine the characterization of the biosorbent material *Ulva Lactuca* and *Sargassum detifolium* and the nature of the biomasses (U and Th).

3.1. Chemical Analysis

Selected samples from Felsite dykes were chosen to carry out biosorption uptake of U and Th. the biosorbent material *Ulva Lactuca* and *Sargassum detifolium*) were used for this work and lead to decreasing of U and Th content (see tables 3, 4, 5 & 6 and figures 1 & 2).

3.1.1. Ulva Lactuca

Table 3 showed the chemical analysis of U in ten samples. Sample 2, U content was 261 ppm *Ulva Lactuca* can capture about 91% of U content. Sample 3, characterized by low U content about 136 ppm *Ulva Lactuca* capture about 82%. In the same way samples 5, 7, 11 and 14, characterized by its low content of U inspired of that *Ulva Lactuca* has the ability to devilish all the U from its content. Samples 5, 7, 11 and 14, *Ulva Lactuca* varied from its capability of dissolving U. On the other hand samples 6 & 12, show moderate amount of dissolving U content about (160, 211) ppm *Ulva Lactuca* has taken about 77% for sample 6 & 80% for sample 12. *Ulva Lactuca* cannot deal with it; it reaches the maximum adsorption capacity; in samples, 1 & 4 it regards to the high content of U, which cannot deal with it (see tables 3 & 4 and figure 2).

Chemical analysis for Th after the action of the biosorbent material (*Ulva Lactuca*) show high adsorption capacity in samples (2 & 3) about 93%, while samples 5 and 13 show also high adsorption about 88% and 86% but less than 2 and 3. Four samples show two of them same capacity (11 & 12) 84%, while (6 & 10) 82%. In other hand, sample 7, show low adsorption capacity then the other ten samples about 76% (see tables 5 & 6 and figure 3).

3.1.2. Sargassum Detifolium

Chemical analyses for Uranium after the action of *Sargassum detifolium* on the ten samples gave highest absorption effect for U in samples 2, 3, 6, 10, 12 and 13. *Sargassum detifolium* show high adsorption in sample 13 (97%) while samples 2 (261 ppm), 12 (211 ppm), 6 (160 ppm) and 3 (136 ppm) show also high capacity of adsorption of Uranium all about (96%). Action of the biosorbent material (*Sargassum detifolium*) on U takes a moderate adsorption in samples 5 & 11 about (93%, 85 %). The ability of adsorbing of U in samples 7 & 14 show the maximum adsorption by *Sargassum detifolium* about 100% it became (zero) Uranium. Finally, *Sargassum detifolium* vanish the U content both together (see tables 3 & 4 and figure 1).

Chemical analyses for Thorium after action of Sargassum detifolium show a high capability of adsorption in sample 11 about 94%. Sample 7, show high action of adsorption about 81%. Samples 10 & 3, show the same percent of adsorption about 76%, while sample 5, show high degree of adsorption about 78%. The percent of Th adsorption in the reminded sample is almost the same as in sample 2 about 72%, while sample 6 about 73%. At last, sample 13 show lower capacity of adsorption about 70% (see tables 5 & 6 and figure 2).

Table (3): Chemical analysis of U (ppm) of the adsorbate El-Sibai and biosorbent materials.

Sample number	U (ppm) in mother sample	U (ppm) with biosorbent material (*Ulva Lactuca*)	U (ppm) with biosorbent material (Sargassum *detifolium*)
2	261	22	65
3	136	24	38
5	75	0	5
6	160	37	45
7	25	0	0
10	110	22	34
11	74	0	5
12	211	42	54
13	110	20	41
14	50	0	0

Table (4): percent of biosorption for U (ppm) for the adsorbate felsite and biosorbent materials.

Sample number	U (%) with biosorbent material (*Ulva Lactuca*)	U (%) with biosorbent material (*Sargassum detifolium*)
2	91.85	75.1
3	82.3	72
5	100	93.4
6	76.8	71.8
7	100	100
10	80	69.1
11	100	93.8
12	80.1	74.5
13	82	62.8
14	100	100
Biosorption averages	**89.3**	**81.3**

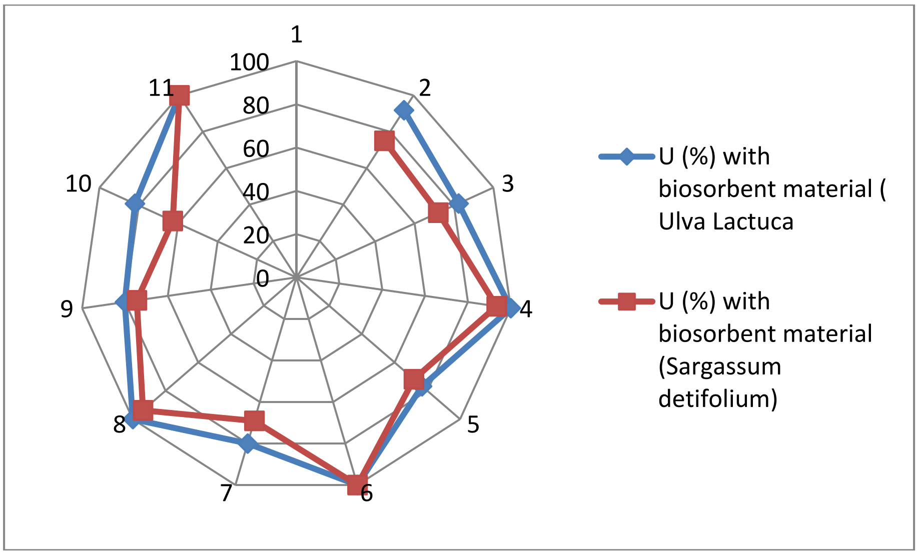

Fig. 1: Histogram shows the capacity of biosorption for U by *Ulva Luctuca and Sargassum detifolium*.

Table (5): Chemical analysis of Th (ppm) adsorbate from the felsite El-Sibai and biosorbent materials.

Sample number	Th (ppm) in mother samples	Th Biosorbent by *Ulva Lactuca*	Th Biosorbent by *Sargassum detifolium*
2	280	40	78
3	200	33	48
5	120	10	26
6	210	36	56
7	70	3	13
10	200	36	47
11	140	0	8
12	290	45	72
13	190	26	56
14	90	7	18

Table (6): Percent of biosorption for Th (ppm) adsorbate from the felsite El-Sibai and biosorbent materials.

Sample number	Th (%) with biosorbent Material(*Ulva Lactuca*)	Th (%) with biosorbent material (*Sargassum detifolium*)
2	85.7	72.15
3	83.5	76.
5	91.6	78.3
6	82.5	73.4
7	95.7	81.4
10	82	76.3
11	100	94.3
12	84.5	75.17
13	86.3	70.5
14	92.3	80
Biosorption averages	**88.4**	**77.8**

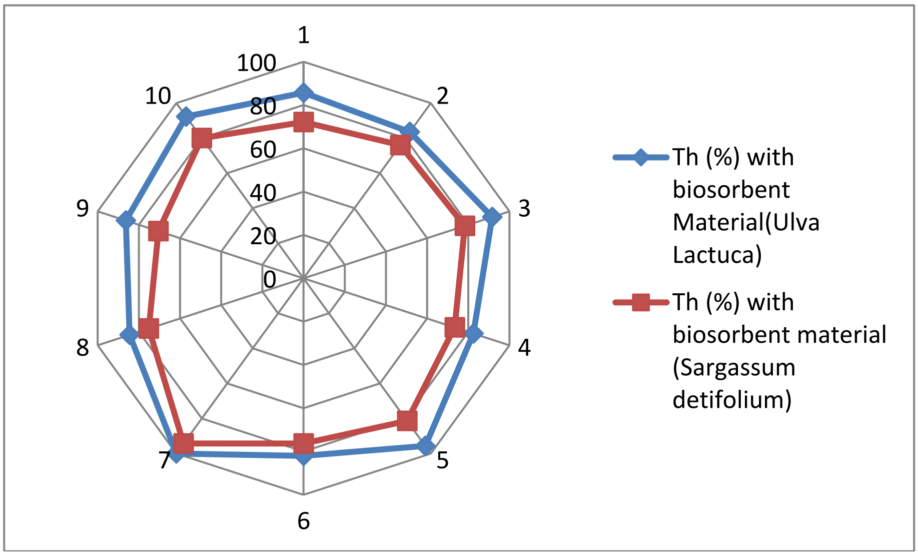

Fig. 2: Histogram shows the capacity of biosorption for Th by *Ulva Luctuca and Sargassum detifolium.*

3.2. Infra Red (IR) Analysis Data

3.2.1. Ulva Luctuca

IR analysis used to determine the characterization of the biosorbent material (*Ulva luctuca)* with the adsorbate El-Sibai felsite (see figures 3 to 10), gave the characteristic wavelength. Sample 2, shows the presence of OH broad, CH aliphatic, SH, CO acidic, CO amide and C-O-C. After treatment with *Ulva luctuca*, SH, CO acidic, CO amide vanished with the appearance of C=C and coupling amide. Mention of using Ulva luctuca with sample 5, four functional groups appeared N-H, OH, C=C, C-O-C and coupling amide. On the other hand, after treatment two functional groups have been appeared CH aliphatic and (alkynes, nitriles with CN triple bond). Sample 6 shows the presence of N-H, CO amide, coupling amide and C-O-C. After treatment, coupling amide and N-H receded from view with the appearance of OH, CH aliphatic and SO_2

(see figures 5 to 8), while sample 7 shows occurring of OH, C=C and C-O-C. After treatment, N-H, CH aliphatic, (alkynes, nitriles with CN triple bond), OH and CO amide have been appeared. Sample 10 treated with *Ulva luctuca* shows the presence of N-H, CH aliphatic, (alkynes, nitriles with CN triple bond), C=C, CO amide and C-O-C. After treatment, C=C, CO amide demise with the appearance of OH and coupling amide. Sample 11 shows the presence of N-H, OH, C=C, CO amide and SO_2 have been receding from view with the appearance of (alkynes, nitriles with CN triple bond) and coupling amide. Sample 13 shows the appearance of N-H and C-O-C. After treatment, N-H demise with the appearance of CH aliphatic and CO acidic. Finally, sample 14 treated with *Ulva luctuca* shows the presence of N-H, OH, coupling amide, CH aliphatic, C=C, C-O-C and (alkynes, nitriles with CN triple bond). After treatment, coupling amide, C=C, N-H and (alkynes, nitriles with CN triple bond) evanescence with the appearance of SH, CO acidic and C-O-C.

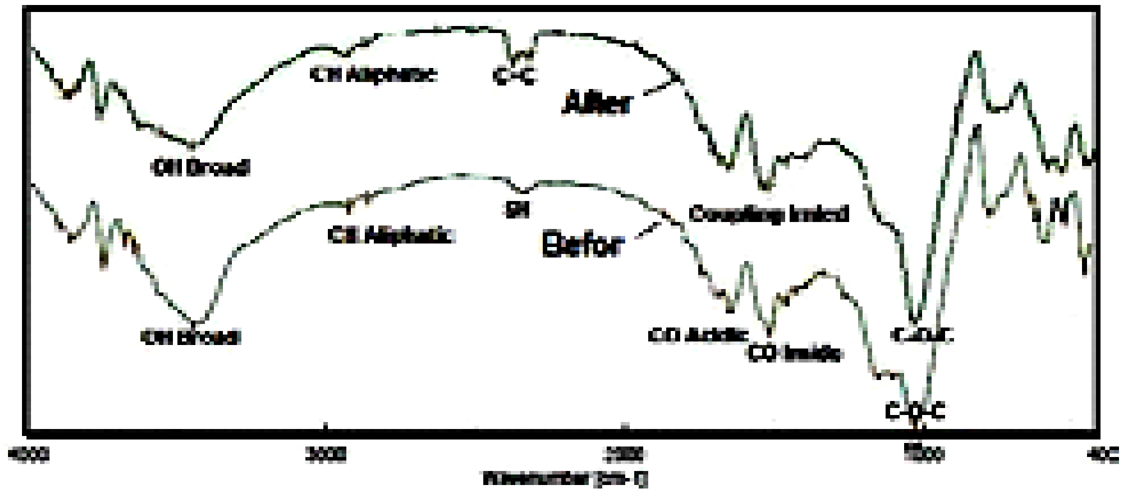

Fig. 3: IR analysis *data* for the adsorbate no 2 with the biosorbent materials *Ulva luctuca.*

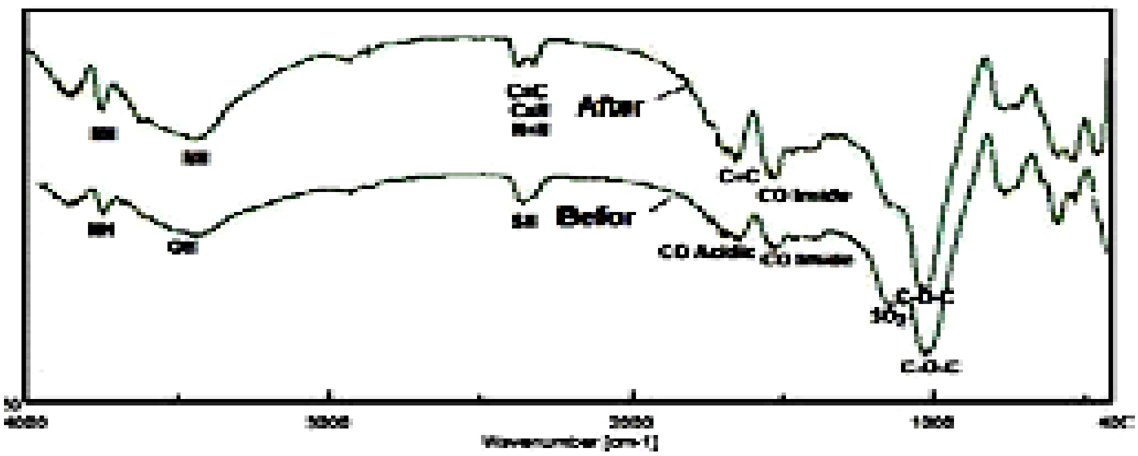

Fig. 4: IR analysis data for the adsorbate no 3 with the biosorbent materials Ulva luctuca.

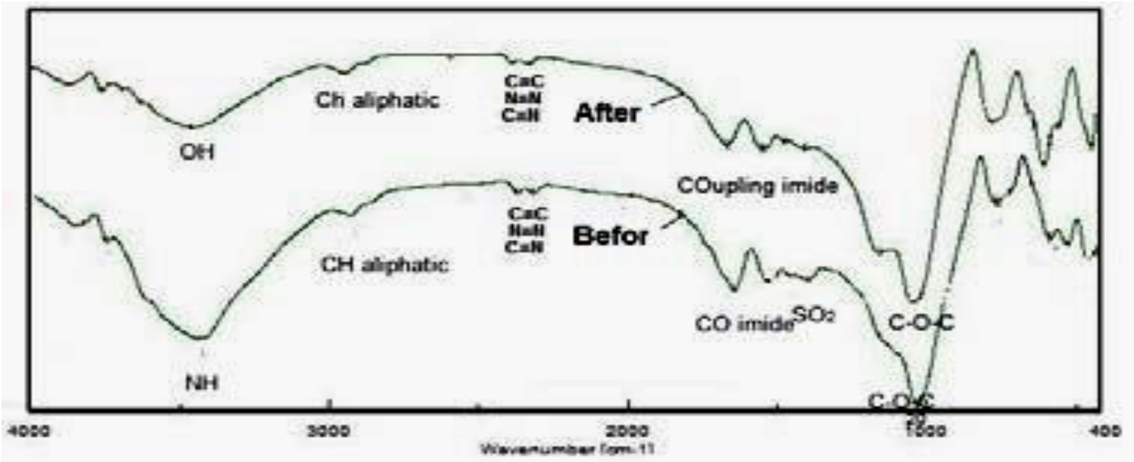

Fig. 5: IR analysis data for the adsorbate no 5 with the biosorbent materials Ulva luctuca.

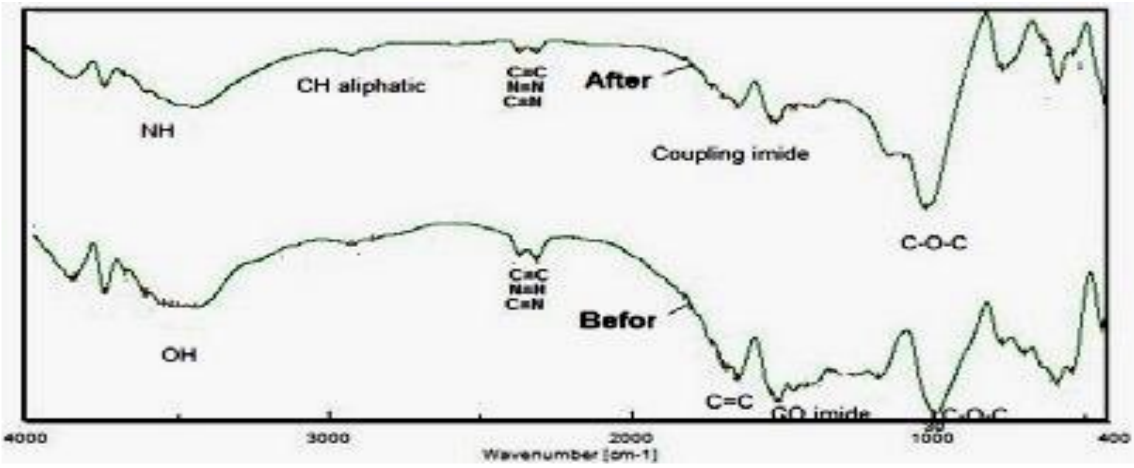

Fig. 6: IR analysis data for the adsorbate no 6 with the biosorbent materials Ulva luctuca.

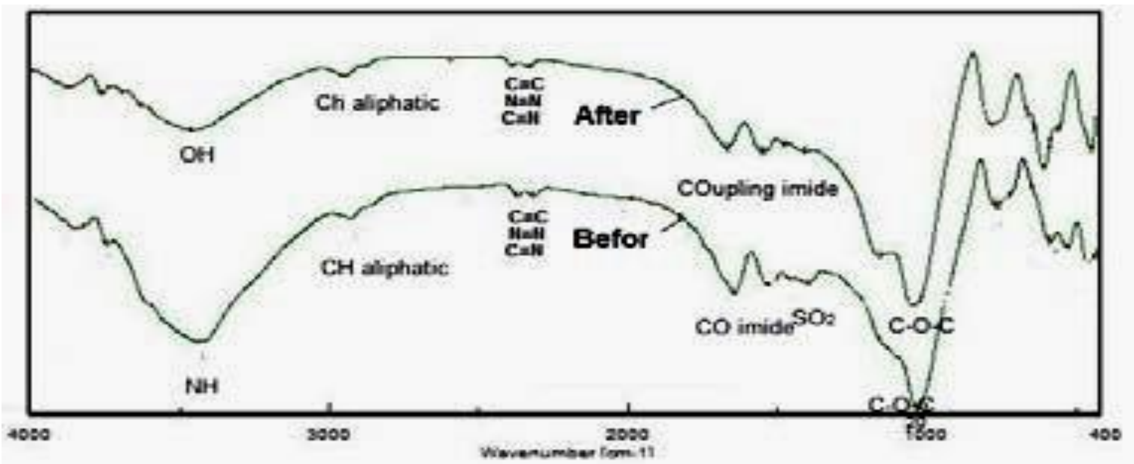

Fig. 7: IR analysis data for the adsorbate no 7 with the biosorbent materials Ulva luctuca.

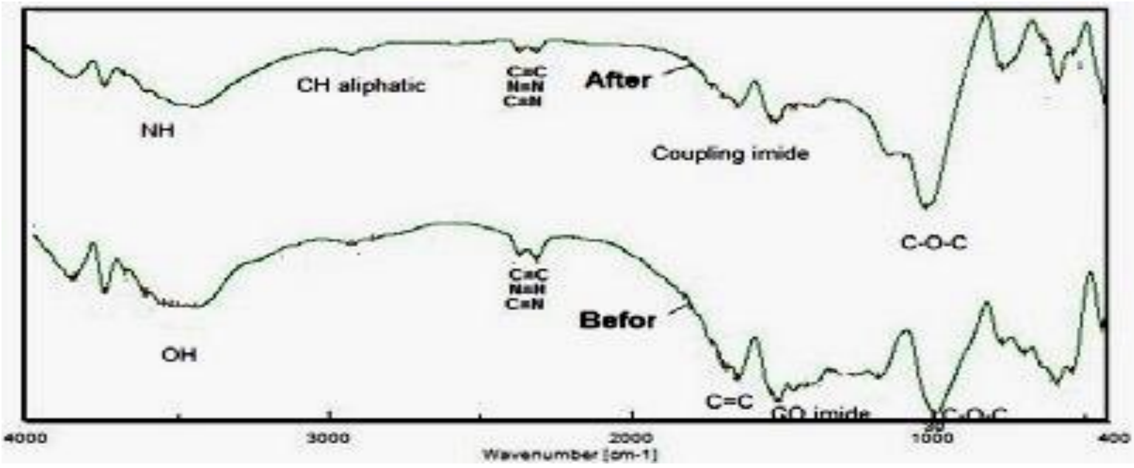

Fig. 8: IR analysis data for the adsorbate no with the biosorbent materials Ulva luctuca.

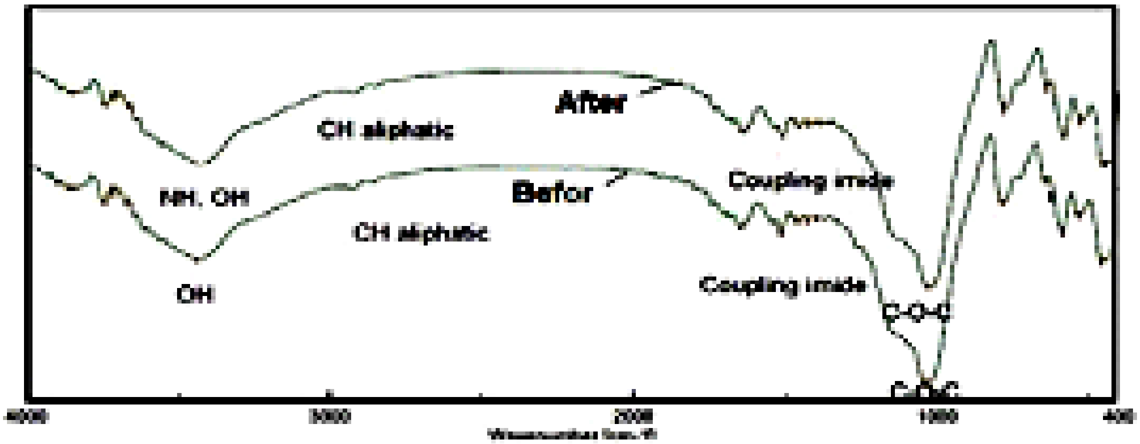

Fig. 9: IR analysis data for the adsorbate no 11 with the biosorbent materials Ulva luctuca.

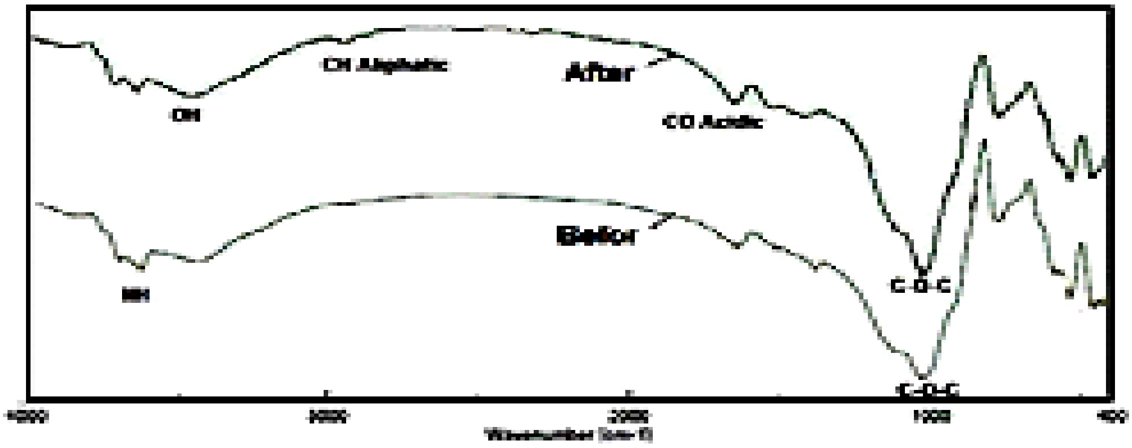

Fig. 10: IR analysis data for the adsorbate no 3 with the biosorbent materials Ulva luctuca.

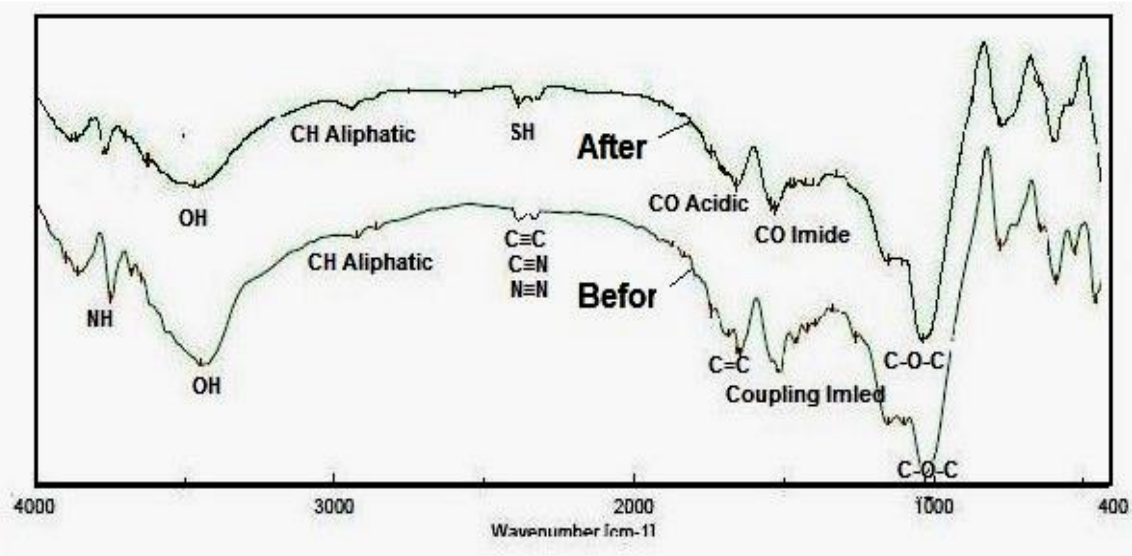

Fig. 11: IR analysis data for the adsorbate no 14 with the biosorbent materials *Ulva luctuca.*

3.2.2. Sargassum Detifolium

IR analysis used to determine the characterization of the biosorbent material (*Sargassum detifolium)* with the adsorbate El-Sibai felsite (see figures 12 to 21) gave the characteristic wavelength. Sample 1 shows different functional groups N-H, CH aliphatic, (alkynes, nitriles with CN triple bond), coupling amide and C-O-C. After treatment, N-H, (alkynes, nitriles with CN triple bond), coupling amide demise with the appearance of C=C, OH and CO amide. Sample 2 treated with *Sargassum detifolium* shows OH, coupling amide, SO_2 and C-O-C. After treatment, coupling amide and SO_2 disappeared with the appearance of N-H, CH aliphatic, (alkynes, nitriles with CN triple bond), C=C and CO amide. Sample 4 treated with *Sargassum detifolium* was mention with high amount of Uranium, shows the presence of N-H, coupling amide and C-O-C. After treatment, N-H and coupling amide receding from view with the appearance of OH, C=C, CO amide and SO_2. Samples 5 and 7 functional groups before treatment with *Sargassum detifolium* are OH, N-H, C=C and C-O-C. After treatment, N-H, C=C evanescence with the appearance of CO amide. Sample 8 shows the presence of OH, CH aliphatic, (alkynes, nitriles with CN triple bond), coupling amide and C-O-C. After treatment, coupling amide demise with the appearance of C=C, SO_2, CO amide. Sample 9 shows N-H, OH, (alkynes, nitriles with CN triple bond), C=C, coupling amide and C-O-C. After treatment, coupling amide disappeared with the appearance of CH aliphatic, SO_2 and CO amide. Sample 10 shows the appearance of N-H, CH aliphatic, (alkynes, nitriles with CN triple bond), CO amide, SO_2 and C-O-C. After treatment, N-H, CO amide, SO_2 vanished with the appearance of OH and coupling amide. Sample 11 treated with *Sargassum detifolium* shows the presence of OH, (alkynes, nitriles with CN triple bond), C=C, CO amide and C-O-C. After treatment, OH, C=C and CO amide evanescence with the appearance of CH aliphatic, N-H and coupling amide. Finally, samples 13 and 14 show the appearance of OH, CH aliphatic, coupling amide and C-O-C. After treatment, N-H.

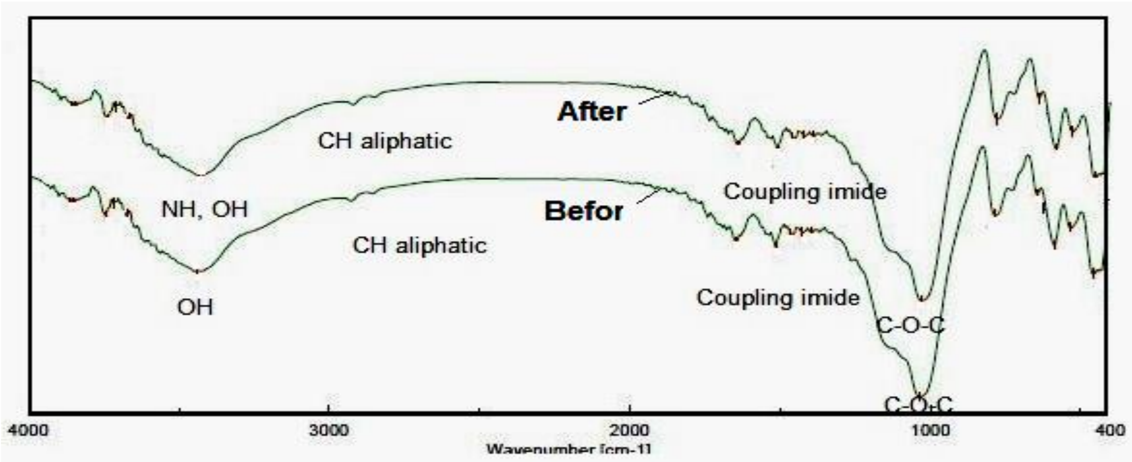

Fig. 12: IR analysis data for the adsorbate no 1 with the biosorbent materials Sargassum *detifolium.*

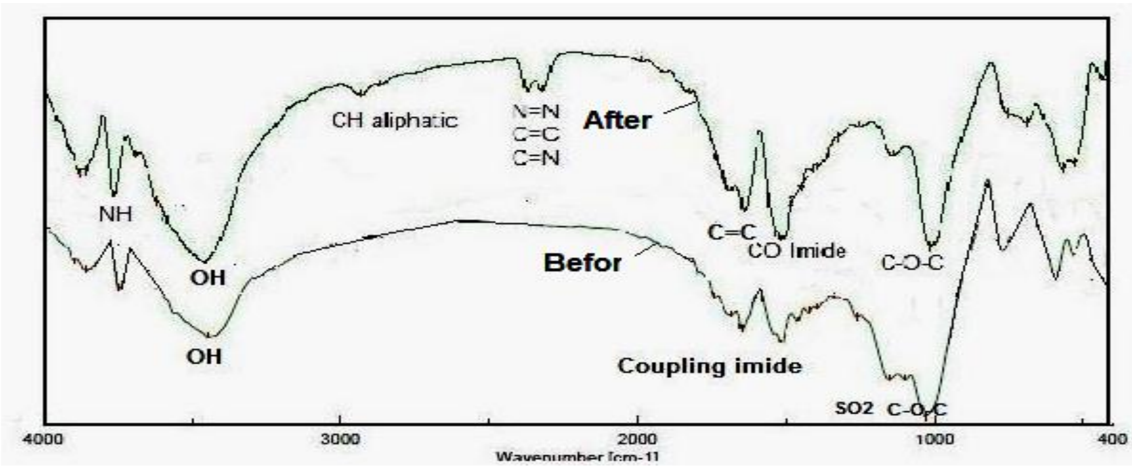

Fig. 13: IR analysis data for the adsorbate no 2 with the biosorbent materials Sargassum *detifolium.*

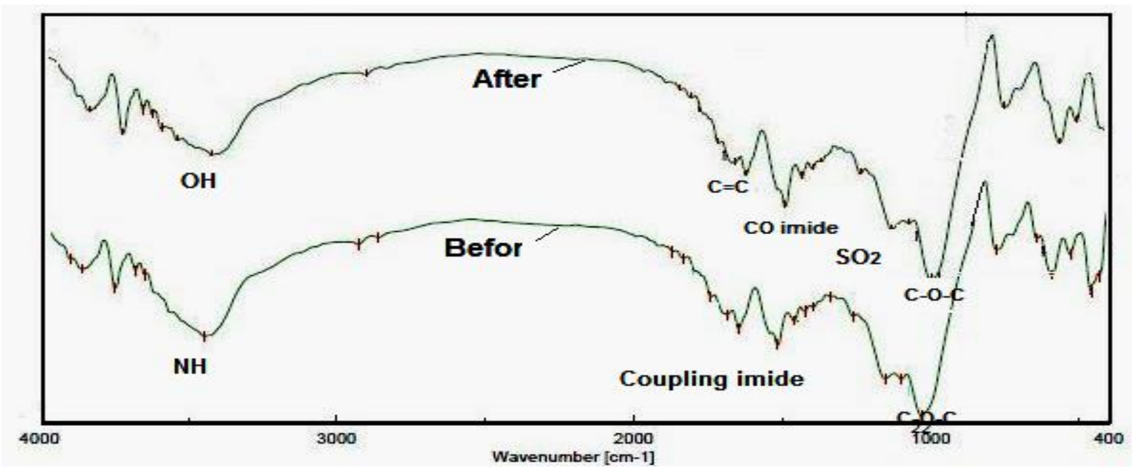

Fig. 14: IR analysis data for the adsorbate no 4 with the biosorbent materials Sargassum *detifolium.*

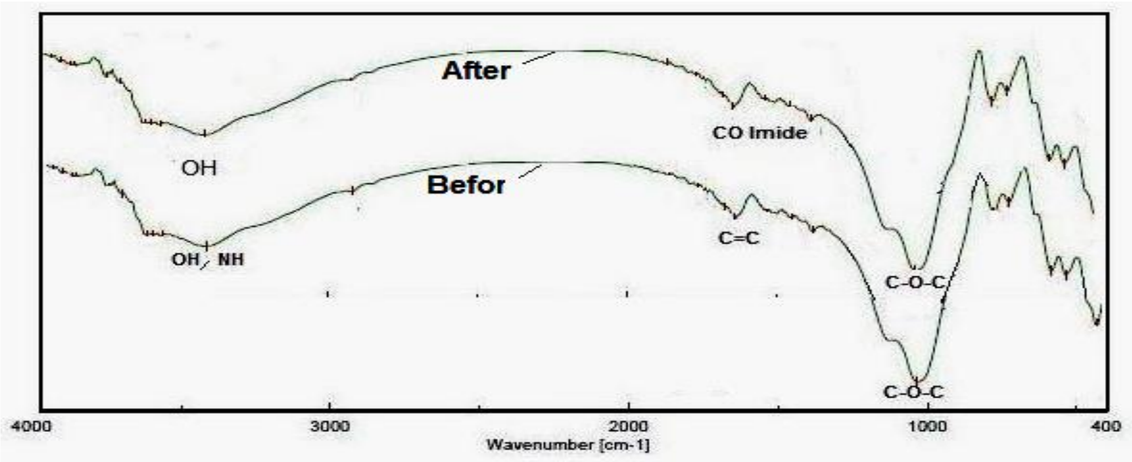

Fig. 15: IR analysis data for the adsorbate no 5 with the biosorbent materials Sargassum *detifolium.*

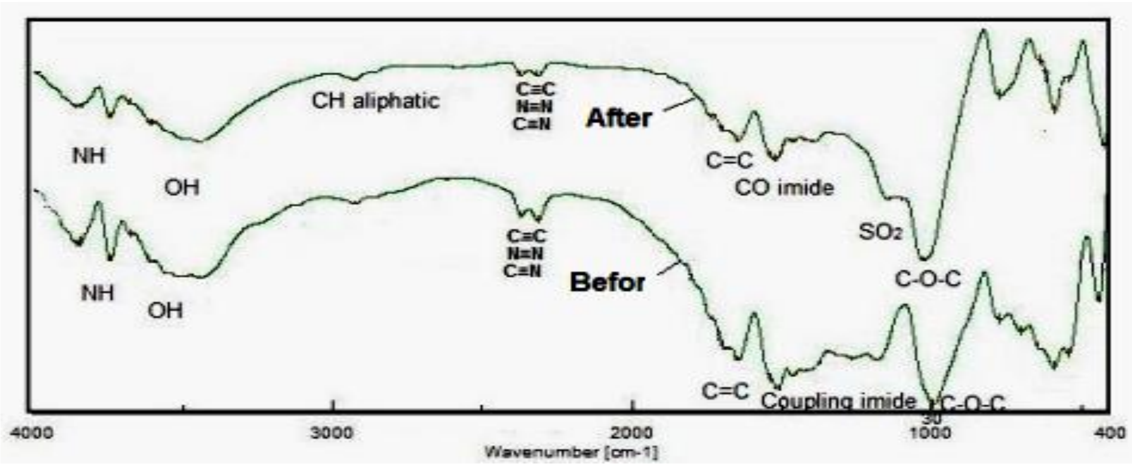

Fig. 16: IR analysis data for the adsorbate no 9 with the biosorbent materials Sargassum *detifolium.*

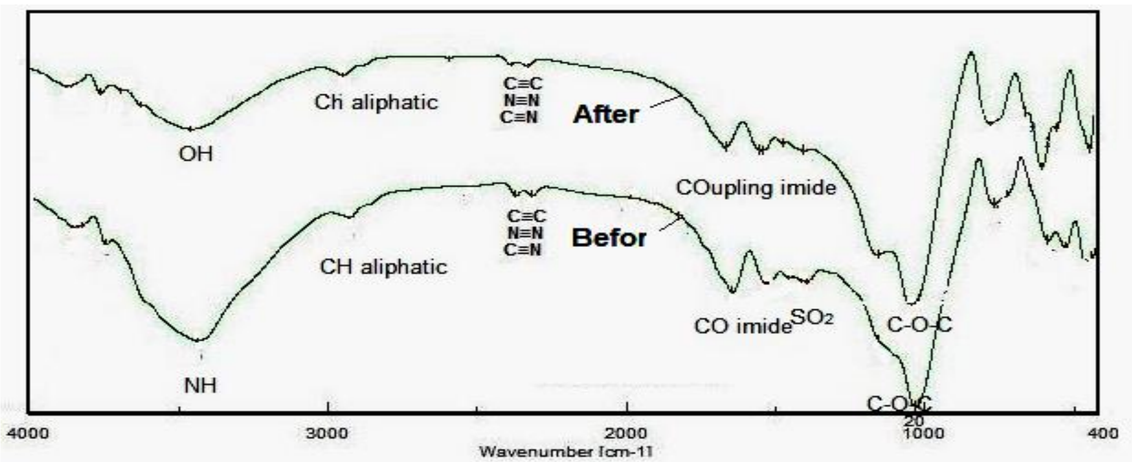

Fig. 17: IR analysis data for the adsorbate no 10 with the biosorbent materials Sargassum *detifolium.*

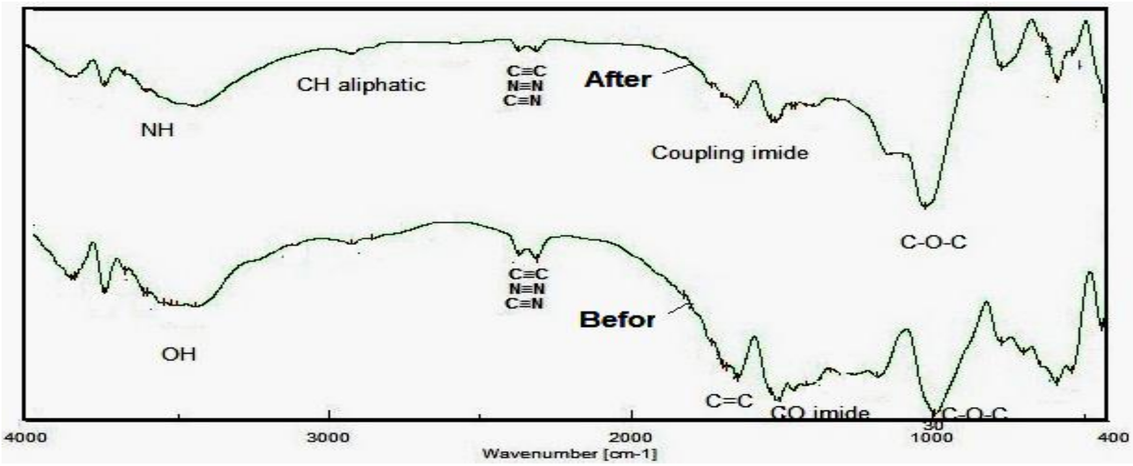

Fig. 18: IR analysis data for the adsorbate no 11 with the biosorbent materials Sargassum *detifolium.*

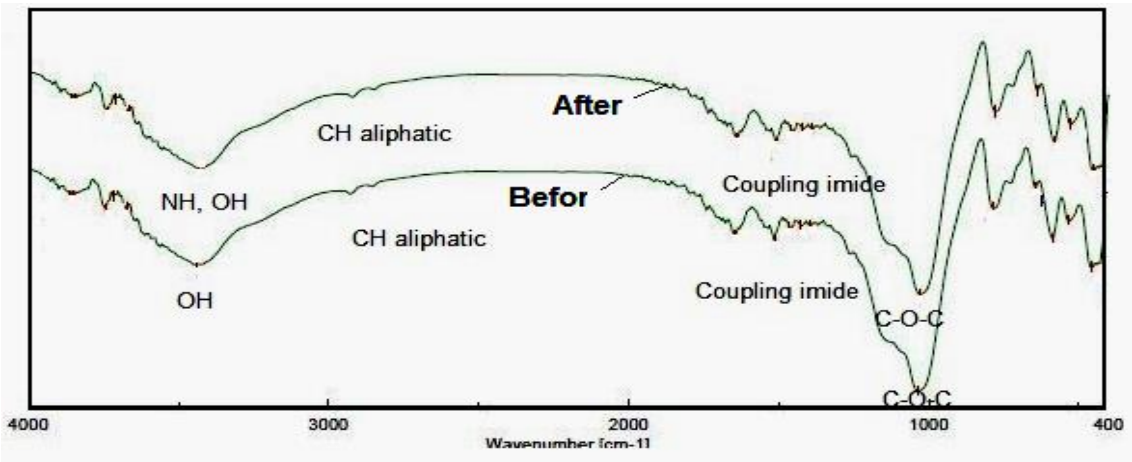

Fig. 19: IR analysis data for the adsorbate no 13 with the biosorbent materials Sargassum *detifolium.*

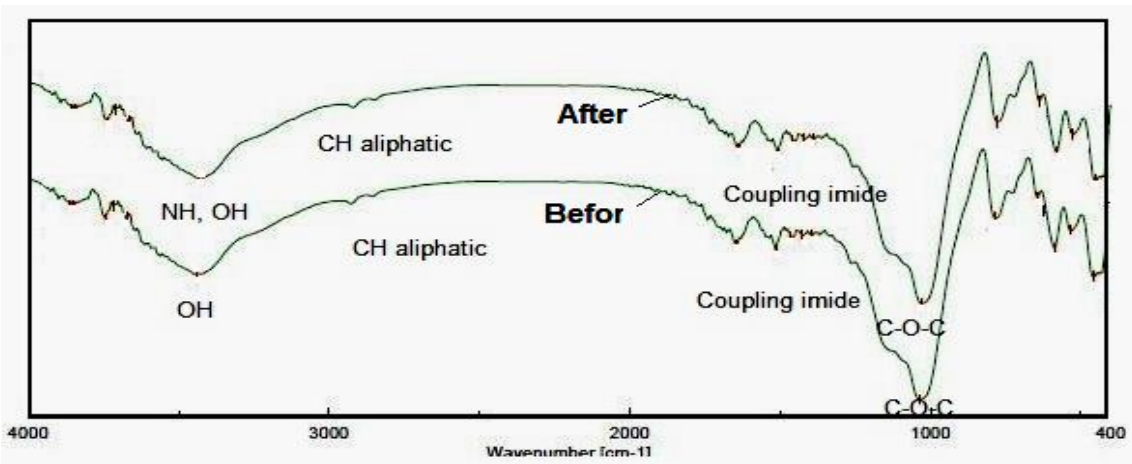

Fig. 20: IR analysis data for the adsorbate no 14 with the biosorbent materials Sargassum *detifolium.*

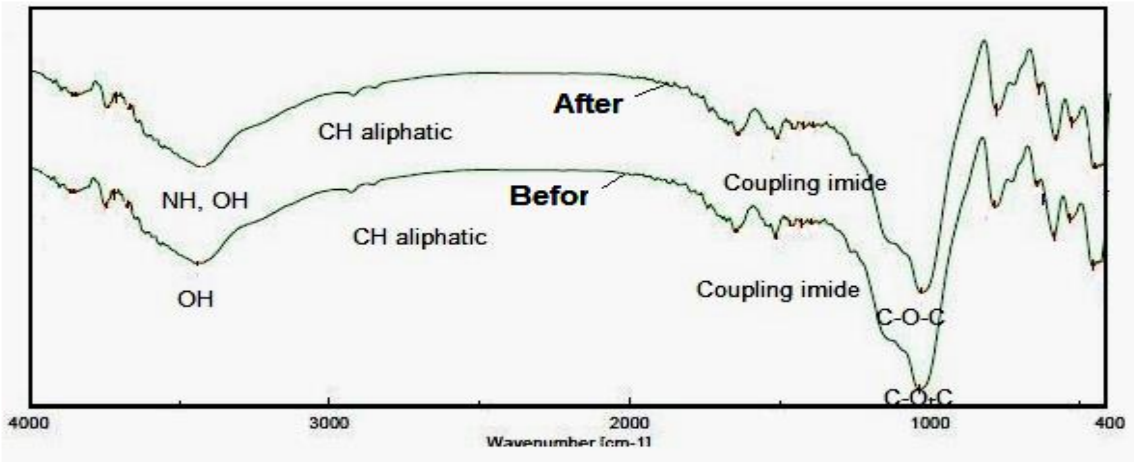

Fig. 21: IR analysis data for the adsorbate no 13 with the biosorbent materials Sargassum.

3.3. Field Emission Gun (FIG) Data Analysis (ESEM)

The environmental scanning electron microscope (ESEM) gave that *Ulva luctuca* adsorb Uranium and Thorium from the sample. Figure 22, the ESEM image and EDX chart for sample of felsite G of El-Saibai area before treatment by *Ulva Lactuca,* shows that the U (Uranophane, $Ca(UO_2)_2(SiO_3OH)_2 \cdot 5H_2O$) content was 32.36%. After treatment, it gave only 0.23% as could be seen in figure 23. While Th content before treatment by *Ulva luctuca* was 34.79% (see figure 24), and after treatment gave 2.11% (see figure 25). *Sargassum detifolium strong* adsorbed Th and U content than *Ulva luctuca* from felsite dykes, before treatment by *Sargassum detifolium* the U (Gummite Ca $(UO_2)_2(SiO_3OH)_2 \cdot 5H_2O$), content was 19.52% (see figure 26) and after treatment gave 00.00% (see figure 27). While Th content before treatment by *Sargassum detifolium* was 18.15% (see figure 28), and after treatment gave 00.00% (see figure 29). The biosorption of Uranium from the uranophane and gummite minerals takes place by using *Ulva luctuca and Sargassum detifolium.* The authors investigate the way of breaking the bonds between the elements using infrared analysis data as given in figures 12 to 21. That indicates the appearance and disappearance of some different functional groups, which act as a carrier for Uranium on the surface of the two algae according to [14]. These data were indicated in EDX of the ESEM by the disassociation of the radioactive minerals (Uranophane, $Ca(UO_2)_2(SiO_3OH)_2 \cdot 5H_2O$) and (Gummite $Ca(UO_2)_2(SiO_3OH)_2 \cdot 5H_2O$) as seen in figures 22 to 29.

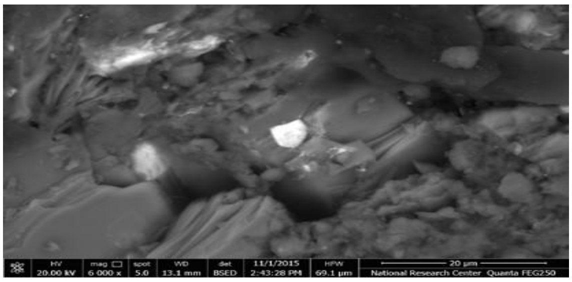

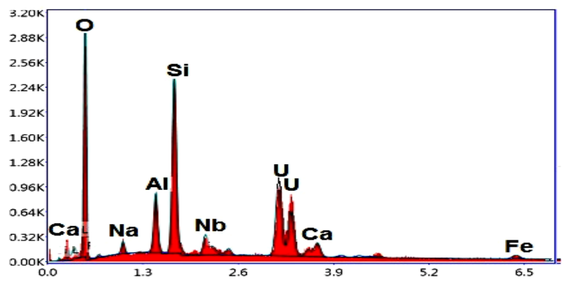

Fig. 22: ESEM image for the adsorbate El-Sibai and EDX chart (for Uranophane), before treatment by *Ulva luctuca* showing high content of Uranium (bright area).

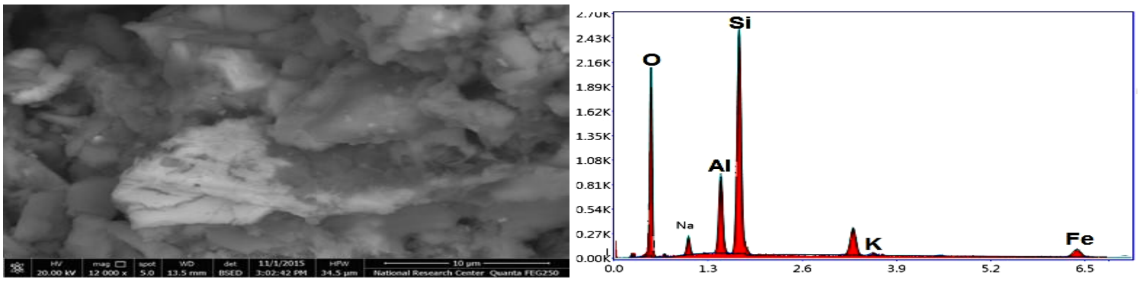

Fig. 23: ESEM image for the adsorbate El-Sibai and EDX chart after treatment by *Ulva luctuca* showing complete biosorption and disappearance of Uranium.

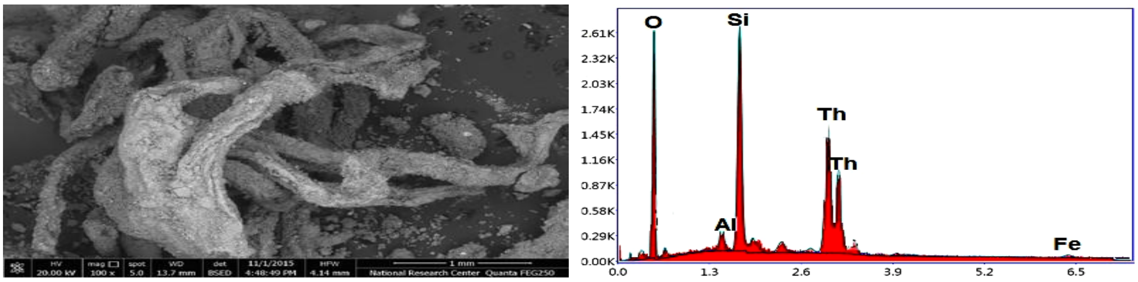

Fig. 24: ESEM image for the adsorbate El-Sibai and EDX chart before treatment by *Ulva luctuca* showing high content of Thorium.

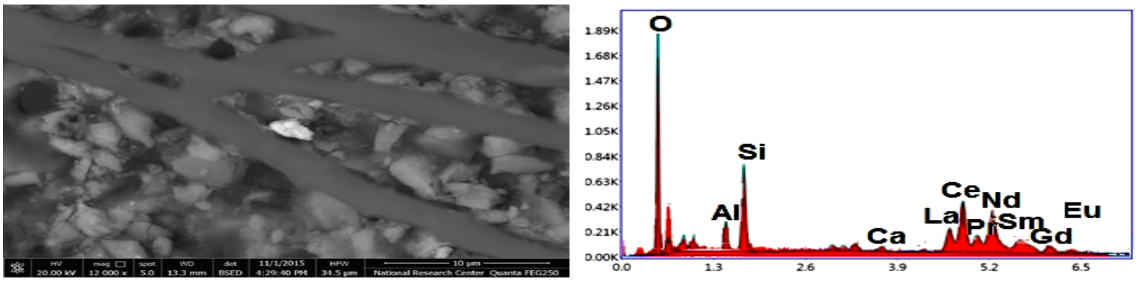

Fig. 25: ESEM image for the adsorbate El-Sibai and EDX chart after treatment by *Ulva luctuca* showing complete biosorption and disappearance of Thorium.

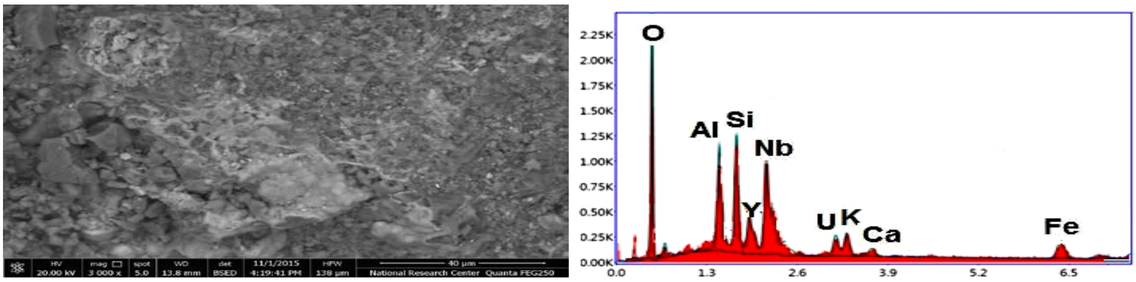

Fig. 26: *ESEM image* for the felsite and EDX chart (Gummite) before treatment by *Sargassum detifolium* showing high content of Uranium.

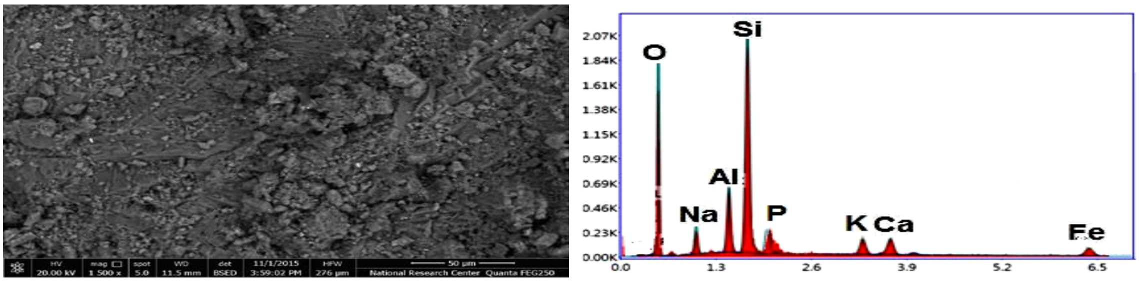

Fig. 27: ESEM image for the adsorbate El-Sibai and EDX chart after treatment by *Sargassum detifolium* showing complete biosorption disappearance of Uranium.

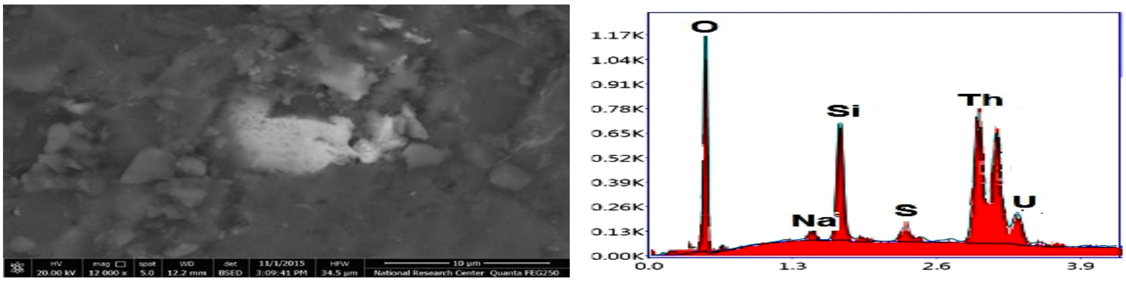

Fig. 28: ESEM image for the adsorbate El-Sibai and EDX chart before treatment by *Sargassum detifolium* showing high content of Thorium.

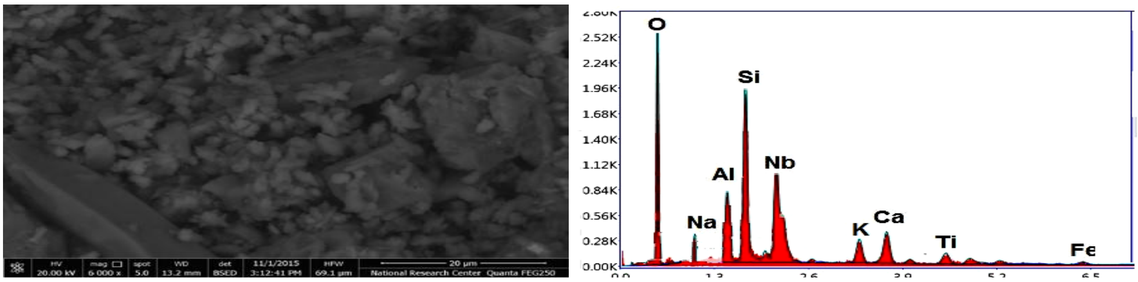

Fig. 29: ESEM image for the adsorbate El-Sibai and EDX chart after treatment by *Sargassum detifolium* showing disappearance of Thorium.

4. CONCLUSIONS

Felsite dykes of El-Sibai area are characterized by a high content of Uranium and Thorium, by using two types of algae as biosorbent materials *(Ulva Lactuca* and *Sargassum detofiulum*). These show that *Ulva Lactuca* as a type of *Rhadophyta* is more active on biosorption of low concentration of Uranium samples, as it give 89% biosorption capacity for U, and 88% for Th, while *Sargassum detofiulum* as a type of *Phyophta absorbed about 81% for Uranium and 77% of Thorium content*. The disassociation of the radioactive minerals (Uranophane, $Ca(UO_2)_2(SiO_3OH)_2 \cdot 5H_2O$) and (Gummite $Ca(UO_2)_2(SiO_3OH)_2 \cdot 5H_2O$), by *Ulva luctuca and Sargassum detifolium* represented by a carrier of different functional group, which carry the Uranium element and lead to broken the bonds between the minerals (Uranophane and Gummite). After biosorption of U on the surface of the algae, this active group acted as carrier of U by the cell of the algae. We can conclude that *Ulva Lactuca* is the best for biosorption of U and Th of Felsite dykes of El-Sibai area than *Sargassum detofiulum*.

Acknowledgment

The authors are grateful to NMA, Egypt to the facilities in laboratory services for this research work.

Conflicts of Interest

The authors report no conflicting interest in any capacity, competing or financial.

5. REFERENCES

[1] Bulgariu, L.; Catalin, B.; Dumitru, and Matei, B.: "Macoveanu valorisation of omanian peat for the removal of some heavy metals from aqueous media", Desalination and Water Treatment, 52: pp. 31-33, (2014).

[2] Gupta, VK. And Rastogi, A.: "Biosorption of lead from aqueous solutions by green algae Spirogyra species: kinetics and equilibrium studies". J Hazard Mater, 152: pp. 407-414, (2008).

[3] Hajar.: "Biosorption of Cadmium from aqueous solution using dead biomass of Brown Algae *Sargassum* Sp: chemical engineering transactions", 17: pp. 1173-1178, (2009).

[4] Kato, K.; Maruta, F.; Kon, N. and Tonouchi, S.: "Distributions and behaviors of C137s and stable Cs in seawater and marine algae on the coast of Niigata Prefecture", Annual Report, Niigata Prefectural Institute of Environmental Radiation Monitoring, Niigata, Japan, (2003).

[5] Kloareg, B.; Demarty, M. and Mabeau, S.: "Ion-exchange properties of isolated cell walls of brown algae: The interstitial solution", Journal of Experimental Botany, 38: pp. 1652-1662, (1987).

[6] Meinrath, A.; Schneider, P. and Meinrath, G.: "Uranium ore and depleted Uranium in the environment, with a reference to Uranium in the biosphere from the Erzgebirge/Sachsen, Germany", Journal of Environmental Radioactivity, 64: pp. 175-193, (2003).

[7] Mohamed, M. A. A.: "Geology, petrology and radioactivity of Gabal El-Sibai area, Central Eastern Desert, Egypt". Ph.D. SC. Thesis, Fac. Sci., Cairo Univ., Egypt, 121 p, (2001).

[8] Noubactep, C.; Licha, T.; Scott, TB.; Fall, M. and Sauter, M.: "Exploring the influence of operational parameters on the reactivity of elemental iron materials", Journal of Hazardous Materials, 172: pp. 943–951, (2009).

[9] Rabie, K. A.; Gad, N. Sh. and Abd-Elfatah, A. I.: "*Ulva Lactuca* and *Sargassum Detofiulum* biosorption susbitibility towards monazite mineral rare earth elements group", Isotope and Radiation Research. 49(1): pp. 139-153, (2017).

[10] Stanley and Byrne: "The influence of solution chemistry on REE uptake by Ulva lactuca L. in seawater", Geochimica et Cosmochimica Acta. 54, 6: pp. 1587-1595, (1990).

[11] Takla, M. A.: "Classification and characterization of the shield rocks of Egypt", 6th international conference on the Geology of Arab World. Cairo University Abstracts. P. xxxii, (2002).

[12] Wang, X. and Dei, R. C. H.: "Kinetic measurements of metal accumulation in two marine microalgae", Marine Biology. 135: pp. 11-23, (1999).

[13] Zeroual, Y.; Moutaouakkil, A.; DzairiF, Z.; Talbi, M.; Chung, P. U.; Lee, K. and Blaghen, M.: "Biosorption of mercury from aqueous solution by *Ulva lctuca* biomass", Bioresource Technology, 90: pp. 349-351, (2003).
[14] Harmsen, K. and deHaan, F. A. M.: "Occurrence and behavior of Uranium and Thorium in soil and water", *Netherlands Journal of Agricultural Science*, 28:pp. 40-62, (1980).
[15] Gad, N. Sh.: "Mechanisms of Uranium and light rare earth elements removal using *Sargassum Detofiulum* as a biosorbent", *J. Bio. Innov. 10(1)*: pp. 300-311, (2021).